



Defence Research and
Development Canada

Recherche et développement
pour la défense Canada



Overview of Wind Gust Modelling with Application to Autonomous Low-Level UAV Control

J. Etele

The scientific or technical validity of this contract is entirely the responsibility of the contractor and the contents do not necessarily have the approval or endorsement of Defence R&D Canada.

Defence R&D Canada – Ottawa

CONTRACT REPORT
DRDC Ottawa CR 2006-221
November 2006

Canada

Overview of Wind Gust Modelling with Application to Autonomous Low-Level UAV Control

J. Etele

Prepared by:

J. Etele, Mechanical and Aerospace Engineering Department, Carleton University
1125 Colonel By Drive, Ottawa, Ontario, Canada, K1S-5B6

Project Manager: Giovanni Fusina 613-998-4720

Contract Number: L5-41768

Contract Scientific Authority: Giovanni Fusina 613-998-4720

The scientific or technical validity of this Contract Report is entirely the responsibility of the contractor and the contents do not necessarily have the approval or endorsement of Defence R&D Canada.

Defence R&D Canada – Ottawa

Contract Report

DRDC Ottawa CR 2006-221

November 2006

Scientific Authority

Original signed by Giovanni Fusina

Giovanni Fusina

Approved by

Original signed by J. Pagotto

J. Pagotto

Acting Head/FFSE Section

Approved for release by

Original signed by C. Boulet

C. Boulet

Head/Document Review Panel

© Her Majesty the Queen in Right of Canada as represented by the Minister of National Defence, 2006

© Sa Majesté la Reine (en droit du Canada), telle que représentée par le ministre de la Défense nationale, 2006

Abstract

The Future Forces Synthetic Environment (FFSE) Section at Defence R&D Canada - Ottawa is currently embarked on an Advanced Research Program entitled “Synthetic Environment Support to Uninhabited Aerial Vehicles (UAVs)”. As part of this project, FFSE has already developed an agile, versatile synthetic environment (SE) tailored toward UAV operations. An enhancement to this SE is being investigated, whereby wind gusts in urban and mountainous environments and their resulting effect on the UAV flight path will be integrated in the FFSE UAV SE. This will give FFSE’s Clients a realistic understanding of the environmental issues associated with UAV operations in urban and mountainous environments and aid in concept of operations development. It will also form the basis of designing control algorithms to alleviate the UAV’s susceptibility to wind gusts. This present study reviews methods available to both quantify a wind gust and use this quantification in the prediction of its effect on UAV stability.

Résumé

La Section des environnements synthétiques des forces de l’avenir (ESFA) de R-D Canada - Ottawa est présentement engagée dans un programme de recherche avancée appelé “soutien en matière d’environnements synthétiques pour les véhicules aériens télépilotés (VAT)”. Dans le cadre de ce projet, la Section ESFA a déjà élaboré un environnement synthétique (ES) agile et souple adapté aux opérations des VAT. On étudie une amélioration possible de cet ES dans laquelle les rafales de vent en milieux urbains et montagneux et leurs effets résultants sur les trajectoires de vol des VAT seront intégrés à l’ES de VAT de la Section ESFA. Cela donnera aux clients de la section un aperçu réaliste des questions environnementales liées aux opérations des VAT en milieux urbains et montagneux et aidera à concevoir l’élaboration des opérations. Cela servira également de base à la conception d’algorithmes de commande visant à atténuer la sensibilité des VAT aux rafales de vent. Cette étude examine les méthodes disponibles pour quantifier une rafale de vent et utiliser cette quantification pour prévoir son effet sur la stabilité d’un VAT.

This page intentionally left blank.

Executive summary

Overview of Wind Gust Modelling with Application to Autonomous Low-Level UAV Control

J. Etele; DRDC Ottawa CR 2006-221; Defence R&D Canada – Ottawa; November 2006.

The current trend towards the increasing use of Unmanned Aerial Vehicles (UAV) has renewed the interest in gust modelling by virtue of the differences between the effects of wind gusts on traditional aircraft and UAVs. Currently, despite advances in modern control theory and application, the primary means of increasing an aircraft's gust resistance is to either make the aircraft 'heavier' (thereby making the aircraft harder to move) or by flying the aircraft higher (thus allowing a larger margin for recovering the previous flight condition). However, for many of the applications for which UAVs are designed these options cannot be implemented. The relative size of most UAVs generally places them under an increased susceptibility to variations in wind conditions, while many of the missions for which these aircraft are used involve flying at low levels and in urban or mountainous environments, where wind gusts are prevalent. Therefore, this report reviews methods available to both quantify a wind gust and use this quantification in the prediction of its effect on UAV stability.

This report contains information relating to the description, modelling, and impact of gusts as they pertain to aircraft. Special attention is given to the nature of atmospheric disturbances near the ground which are of significant importance to low level flying Uninhabited Aerial Vehicles (UAV). Both the details of the most common modelling techniques and the underlying theory are presented so that the reader can both apply the appropriate formulae/equations and modify said equations with reasonable confidence should additional information or methods become available. The three main sections in this report each deal with a specific aspect of the nature of the problem addressed. The first describes the atmosphere in general so that one is able to understand the context in which a gust exists. The second describes the nature of a gust, both in a discrete, single event sense, and as part of the broader spectrum of turbulence in general. The final section relates the modelling of a gust to its incorporation into modern control algorithm design. The approaches suggested in this work will be valuable for the modelling and integration of wind gust effects on a UAV in the FFSE UAV SE.

Sommaire

Overview of Wind Gust Modelling with Application to Autonomous Low-Level UAV Control

J. Etele; DRDC Ottawa CR 2006-221; R & D pour la défense Canada – Ottawa; novembre 2006.

La tendance actuelle vers une utilisation accrue de véhicules aériens télépilotés (VAT) a renouvelé l'intérêt dans la modélisation des rafales en raison des différences entre les effets des rafales de vent sur les aéronefs ordinaires et les VAT. À l'heure actuelle, malgré les progrès de la théorie moderne de la commande et de ses applications, les principaux moyens pour accroître la résistance d'un aéronef aux rafales est de le rendre "plus lourd" (et par conséquent, plus difficile à déplacer) ou de le faire voler plus haut (ce qui offre une marge plus large pour recouvrer la condition de vol précédente). Toutefois, il n'est pas possible d'utiliser ces options dans plusieurs des applications pour lesquelles les VAT ont été conçus. La taille relative de la plupart des VAT les rend généralement plus sensibles aux variations des conditions du vent, tandis que dans plusieurs des types de mission où ces aéronefs sont utilisés, ceux-ci doivent voler à basse altitude et dans des milieux urbains ou montagneux, où les rafales de vent sont courantes. Par conséquent, les présents rapports examinent les méthodes disponibles pour quantifier une rafale de vent et utiliser cette quantification pour prévoir son effet sur la stabilité des VAT.

Ce document contient l'information dirigée à la description, la simulation, et les conséquences des rafales, spécifiquement en relation aux aéronefs. L'effort est surtout porté sur les variations atmosphérique proches de la surface terrestre qui sont très importantes pour les véhicules aériens télépilotés à faible altitudes. Les détails des méthodes les plus utilisées pour les simulations des rafales puis les théories pertinentes sont présentés pour que le lecteur puisse les appliquer ou les modifier avec confiance si l'information additionnelle devrait disponible. Les trois sections majeures dans ce document contient l'information concentrée sur un aspect spécifique du problème étudié. La première décrit l'atmosphère en général pour qu'on puisse comprendre l'environnement dans lequel les rafales existent. La deuxième décrit la nature d'une rafale, comme un événement isolé et comme une partie du phénomène plus grand du turbulence atmosphérique en général. La section finale décrit la simulation d'une rafale et la relation de ces simulations aux méthodes de contrôle modernes. Les approches suggérées dans ce travail seront précieuses pour la modélisation et l'intégration aux ESFA des effets des rafales de vent sur un VAT.

Table of contents

Abstract	i
Résumé	i
Executive summary	iii
Sommaire	iv
Table of contents	v
List of figures	vi
1 The Atmosphere	1
1.1 Geostrophic Wind	1
1.2 Atmospheric Boundary Layer	5
1.2.1 Wind over water	8
2 Types of Modelling	9
2.1 Discrete Gusts	9
2.1.1 Linear Field Approximation	11
2.2 Random Turbulence	13
2.2.1 Power Spectral Density (PSD)	14
3 Application to Aircraft	19
3.1 Four point model	19
3.2 Thunderstorms	21
3.3 Flow past buildings	22
3.4 Control Algorithms	24
References	28
List of Acronyms and Symbols	29

List of figures

Figure 1:	Component of the Earth's rotation vector acting perpendicular to a given latitude on the surface	2
Figure 2:	Direction of the coriolis force at a given Northern hemisphere latitude . . .	3
Figure 3:	Force balance to determine wind direction in the free atmosphere	4
Figure 4:	Wind properties within the boundary layer	6
Figure 5:	A discrete gust modelled using a (1 - cos) shape within a larger continuous turbulence profile	10
Figure 6:	Gust wavelength relative to aircraft size	11
Figure 7:	Superposition of sample frequency components at various ω_j that can be used to reconstruct the actual turbulence profile	15
Figure 8:	Lateral gust velocity psd as per the von Kármán approximation (Eq. 35)	17
Figure 9:	Four points on an aircraft for determining gust gradients	20
Figure 10:	Typical horizontal wind profiles at various altitudes above ground near a thunderstorm	22
Figure 11:	Flows with viscous effects dominant	23
Figure 12:	Flows with inertial effects dominant	24

1 The Atmosphere

In order to properly assess the likelihood of encountering a gust of any given variety, the medium in which these gusts exist must be understood. Therefore, some thought must be given to the Earth's atmosphere and its behavior. As with any fluid medium flowing over a solid object the flow can be divided into two distinct regions, one which can be treated as inviscid (the free atmosphere), and the other where the effects of viscosity cannot be neglected (the boundary layer). This latter region extends to roughly half a kilometer above the surface of the Earth, while the entire atmosphere itself extends to approximately 1,250 km (or about 1% the diameter of the Earth). Above the boundary layer the winds are referred to as geostrophic and flow parallel to the lines of constant pressure (isobars). Within the boundary layer, the flow is generally considered turbulent and is thus dependent to a large extent on the roughness of the surface over which the wind is blowing.

The motions of the atmosphere are complex and can vary according to a number of factors. However, in general one can describe the state of the atmosphere using six variables: (i), (ii) horizontal wind velocities (N-S, E-W); (iii) pressure; (iv) temperature; (v) density; (vi) moisture. This leads to the requirement of six equations to solve for these six unknowns. These are obtained from the principles of mass conservation (for both density and moisture), momentum conservation (Newton's second Law) in both directions parallel to the Earth's surface, energy conservation (the First Law of Thermodynamics), and the equation of state. Although in differential form, provided the six state variables are known at a given time then these equations can be numerically integrated to predict their values at various times in the future (the success, or lack thereof, of this approach can be inferred from the accuracy of modern weather forecasts).

From the point of view of gust impact on aircraft, only the motions of the atmosphere on the microscale are generally of interest (wind patterns on a scale less than 20 km and on time scales less than one hour), however, in general significant weather patterns can extend up to the synoptic scale (scales over 500 km and times exceeding two days, such as the tri-cellular meridional circulation model of the atmosphere).

1.1 Geostrophic Wind

In the upper atmosphere the wind direction can be considered as a balance between the pressure force exerted normal to the isobars and the apparent coriolis force. Although the use of the term may be common, it should be noted that the coriolis *force* exists only due to the rotation of the Earth with respect to a fixed, or inertial, reference frame. In fact, the rotation of the Earth gives rise to a coriolis *acceleration*, which when multiplied by the mass of the air gives rise to an apparent force (from Newton's second Law, $F = ma$). Therefore, similar to an inertial reaction, there is no force in the absence of the coriolis acceleration (which can be expressed as $2\vec{\omega} \times \vec{V}$). Treating the product of a mass times this

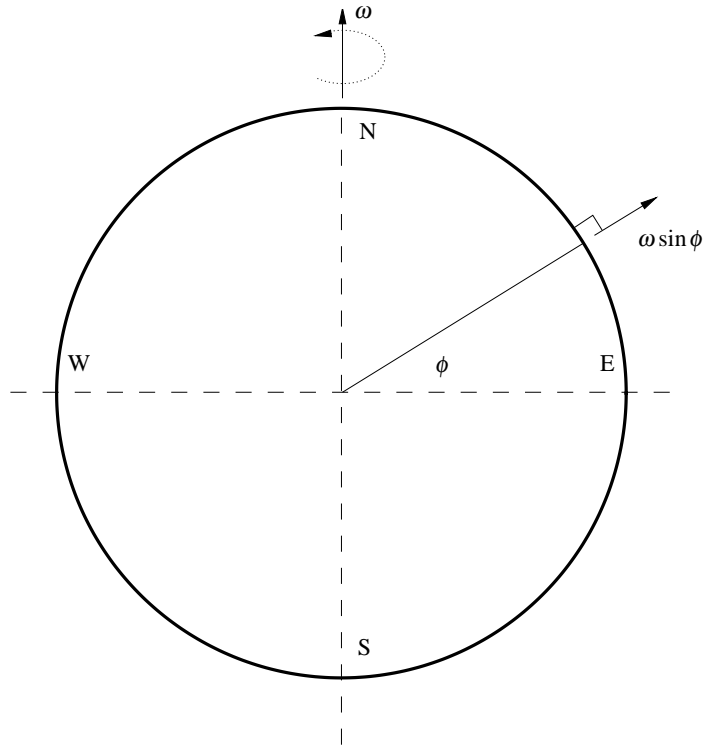


Figure 1:
Component of the Earth's rotation vector acting perpendicular to a given latitude on the surface

acceleration as a force (similar to that exerted by pressure) so that it can be added directly to any force balance equation requires changing the sign so that the coriolis force becomes (using the property of cross products which states $\vec{\omega} \times \vec{V} = -(\vec{V} \times \vec{\omega})$),

$$\vec{F}_c = 2m(\vec{V} \times \vec{\omega}) \quad (1)$$

where \vec{v} is the velocity as measured in the rotating reference frame (i.e., the velocity of the air as seen by observers on the Earth's surface). Since in general we are concerned with geostrophic winds which run parallel to the Earth's surface, the component of Earth's angular velocity acting perpendicular to the surface will depend on the latitude under consideration as shown in Fig. 1. Therefore, for calculating the coriolis force at a given latitude one must replace $\vec{\omega}$ in Eq. 1 with $\vec{\omega} \sin \phi$,

$$\vec{F}_c = 2m(\vec{V} \times \vec{\omega} \sin \phi) \quad (2)$$

To establish the direction of the coriolis force one can use the right hand rule while the magnitude can be found from the definition of the cross product,

$$\vec{V} \times \vec{\omega} = |V||\omega| \sin \beta \quad (3)$$

where β is the angle between the vectors \vec{V} and $\vec{\omega}$ (in this case, if the component $\vec{\omega} \sin \phi$ is used then the angle between this rotation and a velocity parallel to the ground is $\beta = 90^\circ$). Therefore, for a wind initially traveling to the North the coriolis force will act to incline the motion to the East, while for a Southern velocity the coriolis force will act to shift the air to the West (see Fig. 2).

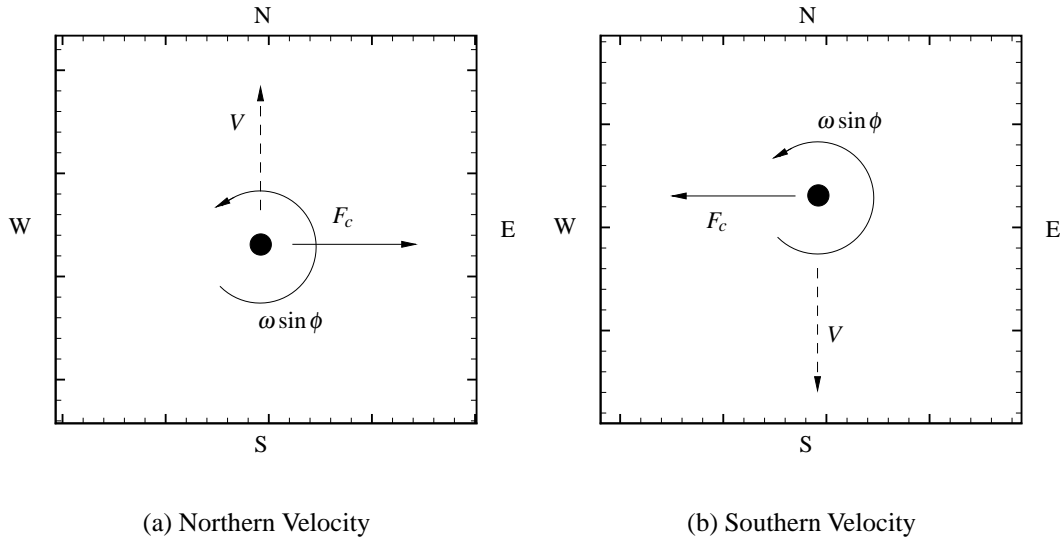


Figure 2: Direction of the coriolis force at a given Northern hemisphere latitude

With the direction of the force established, one can combine Eqs. 2 and 3 to obtain,

$$F_c = 2m|V||\omega| \sin \phi \quad (4)$$

where it is now this force that must balance the pressure force for a constant wind direction to exist. This is illustrated by Fig. 3, where for an air mass initially traveling towards the South due to the pressure gradient, the coriolis force will tend to veer the air mass to the West (Fig. 3(a)). With the air mass traveling in this new direction the coriolis force will change direction to maintain itself perpendicular to both V and $\omega \sin \phi$, thereby continuing to veer the motion towards the West. This process will continue until the velocity is perpendicular to the pressure gradient at which point the coriolis force will exactly balance the pressure force and thus the wind will be traveling parallel to the isobars (Fig. 3(b)).

The only remaining force to be considered in the free atmosphere is that due to the inertial reaction of the air mass traveling along a curved isobar. In this case, in addition to the coriolis acceleration the air will experience a centripetal acceleration acting towards the

centre of curvature (Fig. 3(c)). As with the coriolis effect, one can treat the product of the air mass times the centripetal acceleration as a force, commonly referred to as centrifugal force, $F_r = (mV^2)/r$, where r is the radius of curvature of the isobar. Therefore, for a wind traveling along a curved isobar around a low pressure zone, the centrifugal force acts in the same direction as the coriolis force, while for isobars curved about a high pressure zone the centrifugal force acts counter to the coriolis force (assuming a Northern hemisphere latitude).

Expressing the pressure force as the quotient of the pressure gradient $\partial p/\partial n$ and the density allows the force balance for an air mass as shown in Fig. 3(c) to be expressed as,

$$\frac{\partial p}{\partial n} = \rho \left(2\omega V_{gr} \sin \phi + \frac{V_{gr}^2}{r} \right) \quad (5)$$

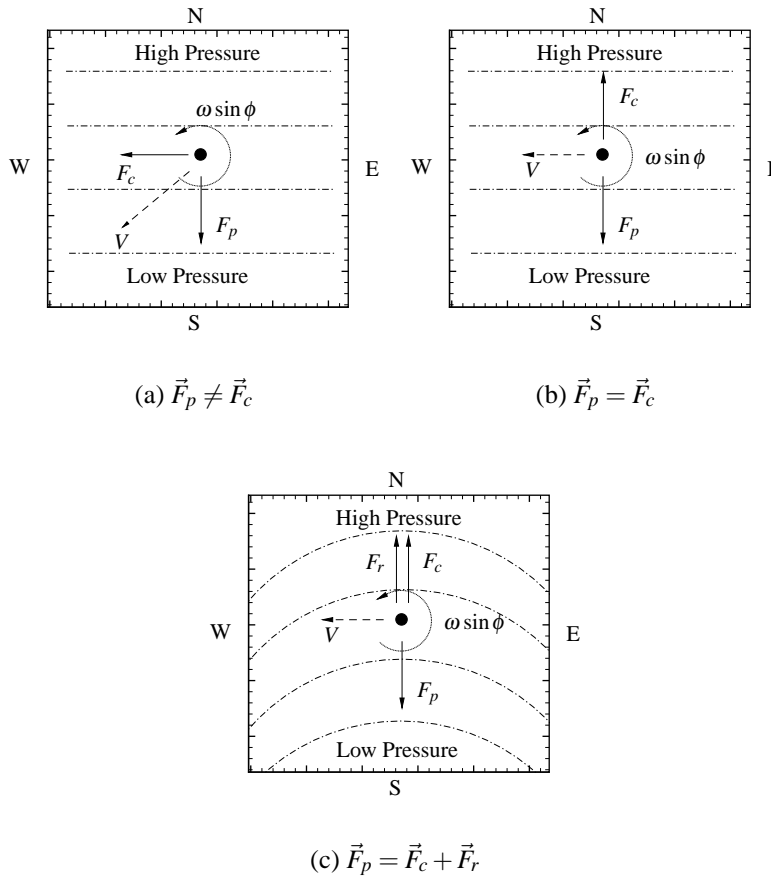


Figure 3: Force balance to determine wind direction in the free atmosphere

which can be used to determine the geostrophic, or gradient, wind velocity (V_{gr}) which flows parallel to the isobars.

1.2 Atmospheric Boundary Layer

Having established a means of calculating both the magnitude and direction of the wind above the boundary layer, it still remains to determine the properties of the atmosphere in the proximity of the Earth's surface. Within the Earth's boundary layer, as with all boundary layers, a force balance in the direction through the boundary layer can be written,

$$\frac{1}{\rho} \frac{\partial p}{\partial z} = 0 \quad (6)$$

If one takes the derivative of Eq. 6 with respect to both x and y (which are the two directions parallel to the surface of the Earth) and assumes that the flow within the boundary layer is incompressible (which is valid for wind velocities less than approximately Mach = 0.2 or 240 km/h), it is possible to conclude that the horizontal wind gradient (both in the x and y direction, therefore $(\partial p)/(\partial n)$) does not vary with altitude. Therefore, using the results for the upper edge of the boundary layer where the wind velocity is related to the pressure gradient through Eq. 5, one can relate the edge velocity (which is simply the gradient wind since above the boundary layer frictional effects can be neglected) to the horizontal pressure gradients within the boundary layer.

However, unlike in the free atmosphere where the wind direction is a balance between the coriolis, centrifugal, and pressure forces acting on the air mass (which leads to a wind flowing parallel to the isobars), in the boundary layer one must also account for the frictional force (Fig. 4(b)) since it is proportional to the change in velocity with height (i.e., $F_{fr} = \mu(\partial V/\partial h)$, Fig. 4(a)). This will cause the wind direction to flow at an angle, α to the isobars (Fig. 4(c)), this angle becoming more severe the closer to the ground the wind is measured (since the frictional force increases as altitude decreases due to the slope of the velocity profile). Therefore, winds generally increase from the ground up, where at some point the frictional force becomes zero and the wind reaches the gradient velocity aligned with the isobars.

The actual shape of the velocity profile as it varies with altitude can be described using theory related directly to the study of turbulent boundary layers. Therefore, dividing the boundary layer into an outer layer and a surface layer, each zone can be described by a profile of a given shape. In the outer layer one can use the defect law to write,

$$(V - V_{gr})/V^* = f\left(\frac{y}{\delta}\right) \quad (7)$$

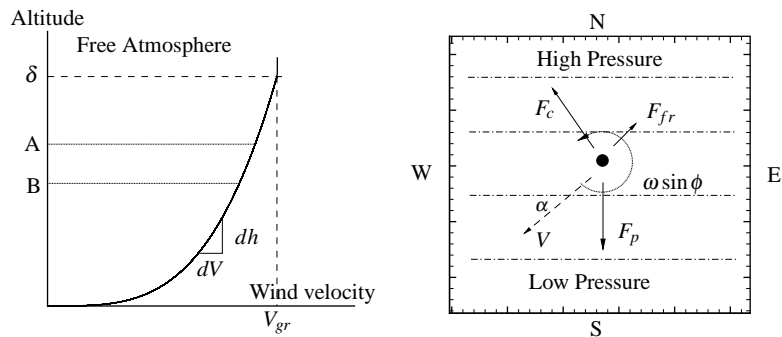
where $V^* = \sqrt{(\tau_{z=0}/\rho)}$ is the friction velocity and is related to the shear stress at the surface,

$$\tau_{z=0} = \mu \left(\frac{\partial V}{\partial h} \right)_{z=0} \quad (8)$$

which is itself a function of the terrain roughness through the value of the co-efficient of friction (μ). In the surface layer the law of the wall can be applied,

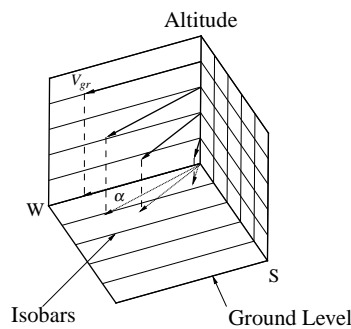
$$\frac{V}{V^*} = f \left(\frac{yV^*}{(\mu/\rho)} \right) = f(y^+) \quad (9)$$

which reduces to the expression $V/V^* = y^+$ in the laminar sub-layer of a turbulent boundary layer. In the overlapping region between these two layers both Eqs. 7 and 9 apply and



(a) Wind profile with height

(b) Force balance in boundary layer



(c) Directional shift with altitude

Figure 4: Wind properties within the boundary layer

thus the mean wind velocity as a function of height can be expressed using the logarithmic law,

$$V(z) = \frac{1}{k} V^* \ln\left(\frac{z}{z_o}\right) \quad (10)$$

where k is the von Kármán constant (approximately 0.4) and z is the height above the surface. The quantity z_o is a roughness length and is directly related to the co-efficient of friction between the air and surface over which the wind is flowing. The expression in Eq. 10 is generally accepted as being valid up to heights of approximately,

$$z_{limit} = b \frac{V^*}{2\omega \sin \phi} \quad (11)$$

where b can range between 0.015 and 0.030. Therefore, by measuring the wind velocity at a given height above the ground and estimating a value for the roughness length (eg. for open terrain $z_o = 0.05$), one can obtain the wind profile up to the height indicated by z_{limit} . At a latitude of 45° , if one measures a 30 kt (15 m/s) wind at a height above ground of 10 m, this can be used to calculate the corresponding friction velocity (using Eq. 10) which in turn can be used in Eq. 11 (assuming a value for b of 0.02) to yield a height of approximately 200 m (\approx 650 ft) over which Eq. 10 can be applied.

Since the relative size of the roughness elements on the ground (i.e. height of trees, buildings, etc.) can be a significant fraction of a low flying aircrafts altitude (unlike the case for most boundary layers where the roughness elements are orders of magnitude smaller than the heights above the surface of interest), an empirical modification is made where z represents not the absolute height above the surface, but rather the height above the “zero plane displacement”, z_d ,

$$z = z_g - z_d \quad (12)$$

where z_g is the height above the ground. Similar to z_o , the zero plane displacement is a function of the nature of the surface (terrain type, roughness elements and their distribution, etc.) and for winds above urban environments can be related to both the general rooftop level (\bar{H}) and the roughness length through,

$$z_d = \bar{H} - \frac{z_o}{k} \quad (13)$$

Typical values of the roughness length for various types of terrain are presented in Table 1.2 taken from Simiu and Scanlan[1].

The relation between the roughness length, which can be thought of as a measure of the turbulent eddy size at ground level, and the surface drag co-efficient can be expressed as,

Table 1: Surface roughness lengths (z_o) and surface drag co-efficients (κ) for various types of terrain (Ref.[1])

Type of Surface	z_o [cm]	κ (10^3)
Sand	0.01 - 0.1	1.2 - 1.9
Snow	0.1 - 0.6	1.9 - 2.9
High Grass	4 - 10	5.2 - 7.6
Pine Forest (mean height 15 m, 1 per 10 m ²)	90 - 100	28 - 30
Sparsely Built-Up Suburb	20 - 40	10.5 - 15.4
Densely Built-Up Suburb	80 - 120	25.1 - 35.6
Large City Centres	200 - 300	61.8 - 110.4

$$\ln(z_o) = \ln(10) - \frac{k}{\sqrt{\kappa}} \quad (14)$$

1.2.1 Wind over water

In the case of winds flowing over water surfaces an additional complication is introduced in that the relative “surface roughness” becomes a function of the state of the waves, which themselves are a function of the wind speed. An empirical relation between the wind speed 10 m above the mean water level and the surface drag co-efficient has been proposed by Amorocho and deVries [2] which applies to wind speeds up to 40 m/s (\approx 80 kts),

$$\kappa = \frac{0.0015}{1 + e^{\frac{12.5 - V(10)}{1.56}}} + 0.00104 \quad (15)$$

The value obtained from Eq. 15 can be used with Eq. 14 to obtain the roughness length for use in calculating the wind velocity as a function of height as per Eq. 10.

2 Types of Modelling

The subject of gust modelling plays an important role in both the design and certification of modern aircraft. From a design point of view, there are two distinct perspectives in terms of the effect of a gust. The first is the effect of a gust encounter on the flight path or orientation of the aircraft. Effective design of auto-pilot or stability augmentation systems requires an accurate assessment of dynamic aircraft behavior. For improved gust response this necessitates an accurate simulation of the types of gusts expected to be encountered, as the effectiveness of control inputs is inherently limited by the fidelity of the gust model considered.

The second perspective relates to structural limitations of the aircraft, where the impact of a gust encounter on the major loads seen by the structure must be accounted and designed for. A static load analysis requires a simpler modelling of the gust, as regulations are related to maximum loads experienced during operation and not the manner in which these maximums are developed. However, when considering the dynamic motion of an aircraft where the frequency content of a given gust can play an important role in the excitation of certain natural frequencies in the structure, a more detailed gust model is required (or rather the idea of turbulence must be considered).

2.1 Discrete Gusts

The standards for evaluating the effects of gusts on an aircraft structure are outlined in FAR Part 25.341. To determine the loads experienced by an aircraft, the current practice is to approximate a discrete gust (which can be considered a single representative section of the broader spectrum of continuous turbulence, see Fig. 5) using a one minus cosine approximation. In this case, the gust velocity is defined as,

$$U(s) = \frac{1}{2}U_{ds} \left[1 - \cos\left(\frac{\pi s}{H}\right) \right] \quad (16)$$

where s [ft] is the distance the aircraft has penetrated into the gust and H [ft] is the distance from the start of the gust to the point at which the gust velocity reaches a maximum. The value U_{ds} is the design gust velocity which varies in strength with altitude in a manner specified by the regulations through the reference gust velocity U_{ref} (56 ft/s at sea level). This design gust velocity is a function of both the shape of the gust through H , and the aircraft design itself through the flight profile alleviation factor, F_g (this last parameter is used to account for the fact that different aircraft configurations will react differently to the same gust),

$$U_{ds} = U_{ref} F_g \left(\frac{H}{350} \right)^{\frac{1}{6}} \quad (17)$$

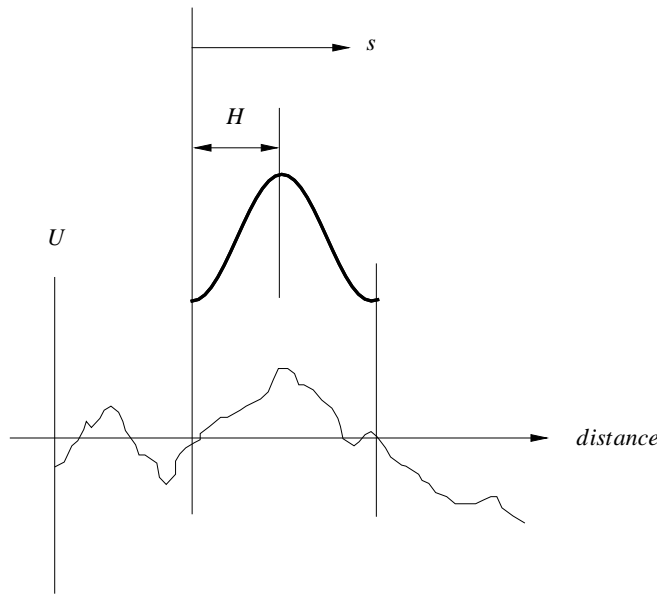


Figure 5: A discrete gust modelled using a $(1 - \cos)$ shape within a larger continuous turbulence profile

This profile must be used in a dynamic analysis since the gust gradient can have a significant impact on the dynamic loads experienced. This leads to the concept of a tuned discrete gust analysis, where numerous gust shapes are considered (i.e. values of H are varied to represent both sharp edged gusts (low values of H) to more gradual gust build-ups (larger values of H)). However, from a static loads point of view, the increase in the load factor caused by the gust is calculated based simply on U_{ref} (assuming the lift acts approximately normal to the aircraft),

$$\Delta n = K_g \left(\frac{\rho U_{ref} V_{cruise} c_{L\alpha}}{2(W/S)} \right) \quad (18)$$

The factor K_g (which is always less than unity) acts to alleviate the effect of the gust by accounting for aircraft motion and the lag effect between the moment the aircraft encounters the gust and the subsequent alteration of the lift generated by the aircraft,

$$K_g = \frac{0.88\mu}{5.3 + \mu} \quad (19)$$

where μ is a non-dimensional fraction relating the aircraft weight to a representative weight of surrounding air that would occupy approximately the same volume as the wing.

In both cases, it can be seen that the actual effect of the gust is not simply taken as immediate, but rather efforts are taken to make the gust profile more representative of what is seen in practice and to model the delay in the aircraft response.

2.1.1 Linear Field Approximation

Although sufficient in terms of certain structural requirements, the above gust approximation applied at a single point on the aircraft (i.e. the location at which s is measured, often taken as the aircraft nose or centre of mass) is often insufficient for accurately predicting effects on the flight profile. This stems from the fact that for gust wavelengths that are large in comparison with the aircraft itself (Fig. 6), the variation in the gust velocity along any of the three spatial dimensions creates an effective rolling moment. For the previously considered gust which can be represented as,

$$g = [u_g, v_g, w_g]^T \tag{20}$$

one can assume this vector to act at the aircraft centre of mass and thus subtract it directly from the aircraft airspeed to obtain the velocity relative to an Earth fixed reference frame (note: a positive gust acts along the positive directions of u , v , and w),

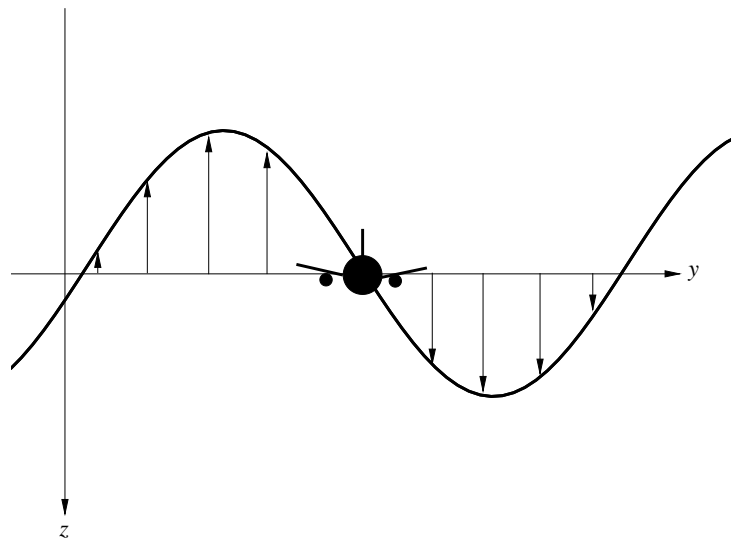


Figure 6: *Gust wavelength relative to aircraft size*

$$\begin{aligned}
u^E &= u - u_g \\
v^E &= v - v_g \\
w^E &= w - w_g
\end{aligned}
\tag{21}$$

However, if the wavelength of the gust is large, then locally around the aircraft one can assume a linear variation in the gust velocity. For example, assuming the vertical gust component w_g varies with both x and y , then the actual value of this component at a given location on the aircraft can be expressed as (neglecting the z location as most aircraft are approximately planar, i.e. they lie nearly completely in a single x - y plane),

$$w_g = \frac{dw_g}{dx}x + \frac{dw_g}{dy}y
\tag{22}$$

By comparison, for an aircraft experiencing a pitching motion about its centre of mass at a rate q , the vertical component of velocity created by this motion at a given location away from the y axis passing through the centre of mass is simply $-qx$ (the negative implies the positive z and y axes extend from the centre of mass downwards and towards the right wing respectively) while for a rolling motion p about the longitudinal axis, again, the vertical component of velocity induced by this motion can be expressed as py . Comparing these results to the expression in Eq. 22, one can represent this linear variation in the vertical gust velocity along x and y as components of a rotational gust velocity,

$$w_g = [p_g, q_g]^T = \left[\left(\frac{\partial w_g}{\partial y} \right), - \left(\frac{\partial w_g}{\partial x} \right) \right]^T
\tag{23}$$

Similarly, both $(\partial u_g/\partial y)$ and $(\partial v_g/\partial x)$ can be related to a yawing motion about the centre of mass. The latter gradient is related to the effects of the vertical stabilizer acting a distance l_t away from the centre of mass, while the former follows more closely the analogy made with both q and p where the variation in the longitudinal gust velocity along the wing span can be made equivalent to the effect of a yawing motion since $u = -ry$.

$$r_{g1} = -\frac{\partial u_g}{\partial y} \quad r_{g2} = \frac{\partial v_g}{\partial x}
\tag{24}$$

Since there is no reason *a priori* to assume that these gradients are such that their representative gust yaw rates would be equal, one must either calculate two rates to be added (i.e., r_{g1} and r_{g2}) or neglect one of these two effects. Subtracting these gust rotations from those of the aircraft in still air yields an effective angular velocity for the aircraft,

$$\begin{aligned}
p &= p_{stillair} - p_g \\
q &= q_{stillair} - q_g \\
r &= r_{stillair} - r_g
\end{aligned}
\tag{25}$$

Therefore, the vector representing a gust which varies spatially over the aircraft can be represented by including a rotational gust velocity around the pitch, roll, and yaw axes in addition to an average linear gust velocity taken to act at the aircraft centre of mass,

$$g = [u_g, v_g, w_g, p_g, q_g, r_g]^T \tag{26}$$

Using Eqs. 21 and 25 it is possible to include a linearly varying gust field into the aircraft state variables, which are used in conjunction with various aircraft stability derivatives to determine the forces and moments acting on an aircraft. This method is considered to yield fairly accurate results as long as the gust wavelength is approximately 10 times the span or tail arm of the aircraft.

2.2 Random Turbulence

The idea of a discrete gust as a subset of a much longer and more continuous spectrum of turbulence as in Fig. 5 leads to the conclusion that for calculating aircraft loads, especially those associated with the dynamic behavior of the aircraft (i.e. natural frequencies of the structure, flutter modes, etc.), one cannot rely solely on this approximation. Therefore, it is necessary to consider the entire spectrum of possible gusts that an aircraft may encounter, in order to adequately ensure none of the possible gust frequencies will have an overly adverse effect. The most common assumption is to assume that the turbulence is a stationary, Gaussian, random process. By being stationary this implies that the turbulence is infinite in duration, while the idea of a Gaussian process is related to the probability of obtaining a given gust velocity at a specific time.

If the still air velocity is taken as the reference condition from which a gust is to be measured, then the mean value of any gust component can be taken as zero. About this mean one can calculate the root mean square (rms) value,

$$\sigma_g = \sqrt{g^2} = \sqrt{\lim_{T \rightarrow \infty} \frac{1}{2T} \int_{-T}^T g^2 dt} = \sqrt{\lim_{N \rightarrow \infty} \frac{1}{N} \sum_{i=1}^{i=N} g_i^2} \tag{27}$$

where in the first case the continuous turbulence spectrum is used in the calculation, while in the second a more practical approach is taken (under most circumstances the turbulent gust velocity is sampled at various times and the total number (N) of these discrete values is used to calculate the rms value). The assumption of a Gaussian process implies that the

probability of obtaining a given gust velocity can be expressed by the relation (assuming a mean value of 0),

$$p(g) = \frac{1}{\sqrt{2\pi}\sigma_g} e^{-\frac{1}{2}\left(\frac{g}{\sigma_g}\right)^2} \quad (28)$$

This has important implications as to the calculation of gust loads. Although there exists experimental evidence to suggest that turbulence is not truly a Gaussian process in that gusts of both small and large magnitudes occur more often than predicted by the normal distribution in Eq. 28, the advantage of this assumption is that the statistical characteristics of an aircrafts response can be calculated directly from the statistical characteristics of the gusts themselves. In addition, by allowing for a complete spectrum of possible gusts, both the short period gusts that tend to affect the aircraft elastic modes (i.e., wing twisting/bending) and the longer period gusts which have more influence on the aircraft rigid modes (i.e., Phugoid) are included in this model (as opposed to the discrete gust model, which by definition must be tuned to account for gusts of varying frequency or magnitude).

2.2.1 Power Spectral Density (PSD)

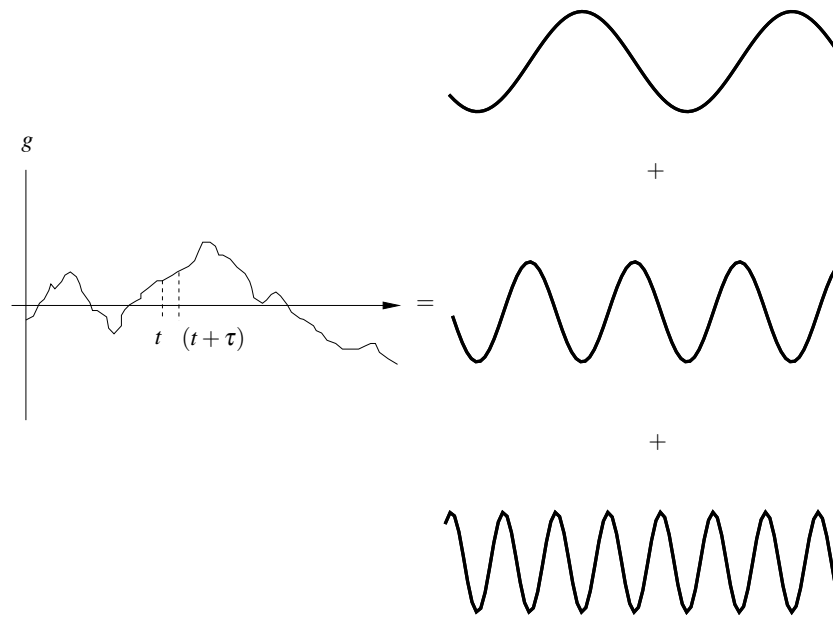
Through Eq. 28 one now has a means of calculating the probability of an aircraft encountering a gust of a given magnitude (g), where the only additional information required is the rms value of the particular gust component under consideration (Eq. 27). However, we are still without a method to quantify the actual turbulence profile. This is accomplished by replacing the turbulence profile with the superposition of an infinite number of sinusoidal components each varying in frequency infinitesimally from one to another. Each component has a specific magnitude which is dependent on the particular frequency,

$$g(t) = \sum_{j=1}^{j=\infty} \sqrt{\Phi(\omega_j)\Delta\omega} \cos(\omega_j t + \psi_j) \quad (29)$$

where $\Phi(\omega_j)$ is referred to as the power-spectral density. Each sinusoidal component is randomly phased relative to all the others by an angle ψ_j , where the probability of obtaining a given value of ψ_j is equal over the entire range 0 to 2π (i.e., it is not Gaussian). This process is shown in Fig. 7 using only a small number of components, the actual psd contains contributions from all values of frequency from zero to infinity. This superposition process is very similar to a Fourier sine series, although in this case each of the frequencies is infinitesimally spaced while in a Fourier series the various components are at discrete intervals of frequency (although there are still an infinite number of components in both cases).

Since $\Phi(\omega)$ is a continuous function of frequency, the psd contains the entire frequency content of the turbulence structure and thus ensures that all possible gusts are considered

Figure 7:
*Superposition
of sample
frequency
components at
various ω_j that
can be used
to reconstruct
the actual
turbulence
profile*



in any analysis with which this is used. The psd can be directly related to the rms value of the gust, where $\Phi(\omega)d\omega$ is the contribution to σ_g of the components with a frequency between ω and $\omega + d\omega$ making the rms value the area under the psd curve,

$$\sigma_g^2 = \int_{-\infty}^{\infty} \Phi(\omega)d\omega \quad (30)$$

Note: the psd is shown as two sided in that it exists for both positive and negative values of frequency. For a one sided spectrum (i.e., the integration is performed from zero to infinity) the psd would be twice that obtained in Eq. 30

Therefore, with a psd one can re-create any given stationary, random, Gaussian process and thus for every experimental turbulence profile measured that matches this description, one can calculate a corresponding psd. This is often accomplished using the autocorrelation function,

$$R_{ij}(\vec{\xi}, \tau) = \overline{g_i(\vec{r}, t)g_j(\vec{r} + \vec{\xi}, t + \tau)} \quad (31)$$

where the vector $\vec{\xi} = \sqrt{(\Delta x^2 + \Delta y^2 + \Delta z^2)}$ for a Cartesian co-ordinate system and τ is a time increment on the scale of the motion of the aircraft.

In addition to the above mentioned assumptions, if one adds that the turbulence can be treated as frozen in space (i.e., in the time it takes for an aircraft to traverse a given turbulence field, the velocities have not had sufficient time to change significantly), then the various components of turbulence (g_i) become solely a function of position and *not* the large scale time. Therefore $g_i(r, t) \rightarrow g_i(r)$ (this is known as Taylor's hypothesis) and under these circumstances the one dimensional psd can be related to the autocorrelation function as,

$$\Phi_{ij}(\Omega) = \frac{1}{2\pi} \int_{-\infty}^{\infty} R_{ij} \cos(\Omega\xi) d\xi \quad (32)$$

where Ω is the reduced frequency, which is related to the circular frequency through,

$$\Omega = \frac{\omega}{V} \quad (33)$$

For turbulence as described by a stationary, random, Gaussian, frozen, process there are two critical one dimensional psds, corresponding to the lateral and longitudinal directions. In these cases one is primarily concerned with the determination of only $\Phi_{11}(\Omega)$ and $\Phi_{33}(\Omega) = \Phi_{22}(\Omega)$ respectively (requiring only the $R_{i=j}$ terms). For an aircraft passing through a turbulence field at a speed V , or for measurements of turbulence taken on a tower with a mean wind speed equal to V , the relation between distance and time is simply $\xi = V\tau$ (therefore $d\xi = d\tau$) and thus the autocorrelation function in Eq. 31 can be re-written as,

$$R(\tau) = \overline{g(t)g(t+\tau)} = \lim_{T \rightarrow \infty} \frac{1}{2T} \int_{-T}^T g(t)g(t+\tau) dt \quad (34)$$

which for $\tau = 0$ yields the rms value of g .

For typical gusts encountered at altitude there are two main approximations for the psd, the von Kármán and Dryden models, each proposing a separate function for gusts in the longitudinal and lateral directions. Currently, the von Kármán model is specified as the required model in FAR 25 Appendix G which for vertical gusts gives,

$$\Phi(\Omega) = \sigma_g^2 \frac{L}{\pi} \frac{1 + \frac{8}{3}(1.339L\Omega)^2}{[1 + (1.339L\Omega)^2]^{\frac{11}{6}}} \quad (35)$$

To use Eq. 35 one must specify a turbulence length scale L , where Appendix G of FAR 25 sets this value at 2,500 ft (762 m). This value determines the location of the point at which the psd curve starts to slope downwards as shown in Fig. 8. Therefore, the selection of L has a greater influence on the lower frequency spectrum of the psd, which in terms of determining aircraft loads due to gusts tends to be relatively unimportant when compared

to the higher frequencies where the effect of L is minimal. No matter where the curve starts to slope downwards it always reduces to a slope of -5/3 at higher frequencies on a log-log scale, while the actual location of the curve for various values of L can be made to lie along the same path through a variation in σ_g which is a measure of the magnitude of the gust fluctuations ($\sigma_g \propto L^{\frac{1}{3}}$).

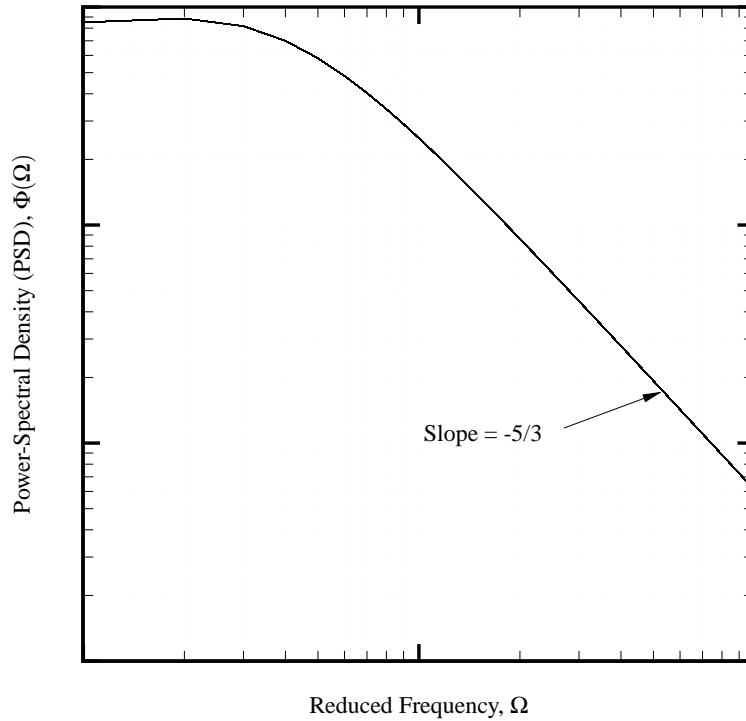


Figure 8:
Lateral gust velocity psd as per the von Kármán approximation (Eq. 35)

As previously mentioned, there is a separate von Kármán psd for longitudinal gusts which can be written,

$$\Phi(\Omega) = \sigma_g^2 \frac{2L}{\pi} \frac{1}{[1 + (1.339L\Omega)^2]^{\frac{5}{6}}} \quad (36)$$

The difference between the two psds lies in the manner in which the gust is seen by the aircraft. For the case of a transverse gust (vertical or lateral), the gust velocity field is seen as a shearing type field with respect to the flight velocity. However, for a longitudinal gust an increase in the wind velocity parallel to the flight velocity must actually be entraining air from the lateral directions to supplement the required mass flow, while for a gust opposing the flight velocity the opposite is true and airflow must be ejected laterally. In either case

the variation in the psd is not due to the turbulence in each direction being different, in fact, for high altitude flight the turbulence is usually assumed to be isotropic (σ_g is the same in all directions). Therefore, the turbulent gust profile is the same independent of the direction under consideration and the differences between Eqs. 35 and 36 are related solely to the orientation of the aircraft with respect to the gust.

3 Application to Aircraft

With both the atmosphere and the gusts within this medium adequately described, it remains to apply the theory, or its relevant components, to situations of importance to aircraft. For instance, if one wishes to use the linear field approximation for a gust, it still remains how to establish this variation so that it relates to the actual situation experienced by the aircraft. Furthermore, even with the gust field represented, it remains to be seen how the aircraft will react under various circumstances.

From a structural point of view, it is the higher frequency disturbances which play a dominant role in exciting the structure and thus create significant gust loading situations. Therefore, under these circumstances the idea of a turbulence spectrum and corresponding psds needs to be considered. However, from a navigational or guidance point of view the opposite is true, where it is the low frequency disturbances which are more important thereby indicating the importance of the discrete or linearly varying gust model. For the purposes of this report since the flight path of a low flying aircraft must be carefully controlled (more so than for traditional aircraft operating altitudes) emphasis will be given to the factors which influence navigation, but this is not to imply that the structural considerations of turbulence can be neglected.

3.1 Four point model

For aircraft traveling through disturbances of various frequencies, a meaningful non dimensional parameter which can be used to characterize the flow is the “reduced frequency” or “Strouhal number”. If a gust varies with a period $T = (2\pi/\omega)$ and travels at a mean speed V (or from the point of view of a stationary gust the aircraft travels through at a speed V), then a distance, or wavelength, can be calculated as,

$$\lambda = \frac{2\pi V}{\omega} \quad (37)$$

Therefore, using the wing half chord as a measure of the aircraft dimension and dividing this by the “gust” wavelength above, one obtains a parameter that is directly proportional to the reduced frequency, k ,

$$\frac{(c/2)}{\lambda} \propto k = \frac{\omega c}{2V} = \frac{\Omega c}{2} \quad (38)$$

In order to consider the aerodynamic forces and moments being applied to the aircraft as steady, it is generally accepted that the reduced frequency must be below approximately 0.1. Above this value there is a significant phase lag in the generation of lift with respect

to wing movement in addition to a reduction in its magnitude. These are common factors which must be considered in a dynamic analysis, where for example in considering flutter Theodorsen's function is often used to represent the unsteady lift generated by an oscillating wing (where the case of steady lift is obtained by allowing $k \rightarrow 0$ thereby effectively eliminating ω since the wing dimension $c \neq 0$ while V has practical upper limits). Under this restriction, the limit on the gust wavelength as compared to the wing chord is,

$$\frac{\lambda}{c} \geq 10\pi \quad (39)$$

which for an aircraft with a tail arm three times the length of the wing chord yields a minimum gust wavelength of approximately 10 times the tail arm. Recalling the section describing a linearly varying gust, this matches the limit imposed on the use of a gust rotational velocity to approximate a linearly varying gust field (see Eq. 26). This indicates that using this method of approximating a gust assumes quasi-steady aerodynamics which is indeed the case.

Since a linear variation in a particular gust component can be related to a particular angular velocity, by measuring the gust velocity at various points on an aircraft separated by a known distance one can obtain the desired gust rotations. This can be done using the "four point model", where the gust components are measured at the four locations shown in Fig. 9.

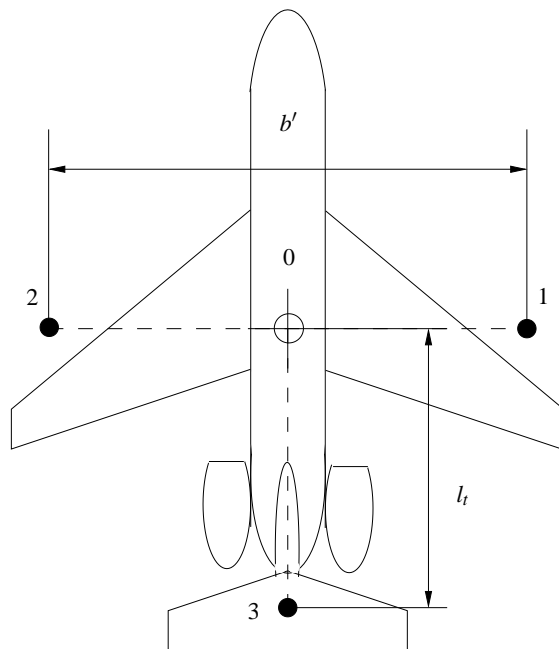


Figure 9: Four points on an aircraft for determining gust gradients

For both the horizontal components of a gust, the value at the centre of mass (point 0 in Fig. 9) is used as the gust component without reference to the other points (i.e., $u_g = u_0$ and $v_g = v_0$) while the vertical component is taken as the average of the three measurements along the wingspan,

$$w_g = \frac{1}{3}(w_0 + w_1 + w_2) \quad (40)$$

As per Eq. 23 the roll and pitch rates associated with the gust are calculated as,

$$\begin{aligned} p_g &= \frac{1}{b'}(w_1 - w_2) \\ q_g &= \frac{1}{l_r}(w_3 - w_0) \end{aligned} \quad (41)$$

while for the two yaw rates one can use Eqs. 24 to obtain,

$$\begin{aligned} r_{g1} &= \frac{1}{b'}(u_2 - u_1) \\ r_{g2} &= \frac{1}{l_r}(v_0 - v_3) \end{aligned} \quad (42)$$

In this manner one now has the complete gust vector which can be used as a disturbance vector in calculating the trajectory of an aircraft assuming a linearly varying gust. This method is based on one proposed by Holley and Bryson [3], where the value for b' is recommended as 85% of the wingspan.

From a structural point of view, the measurements taken on these four points of the aircraft can be related to the autocorrelation function defined in Eq. 34 by noting that in a time τ the aircraft (and hence any of the given points) has translated a distance equal to $\xi = V\tau$ and thus the autocorrelation function can be expressed as (using the gust roll rate, p_g , as an example),

$$R_{pp}(\tau) = \overline{p_g(t)p_g(t+\tau)} = \frac{1}{(b')^2} \overline{(w_1w'_1 - w_1w'_2 - w'_1w_2 + w_2w'_2)} \quad (43)$$

where the primed variables are those measured at the time $(t + \tau)$.

3.2 Thunderstorms

Although there are numerous sources of turbulence, one of the most common is the thunderstorm. Since storms are not stationary, unlike turbulence caused by terrain roughness, thunderstorm turbulence can be a cause of concern for aircraft operating at any location. Typically characterized by significant wind shear in addition to strong vertical up/down

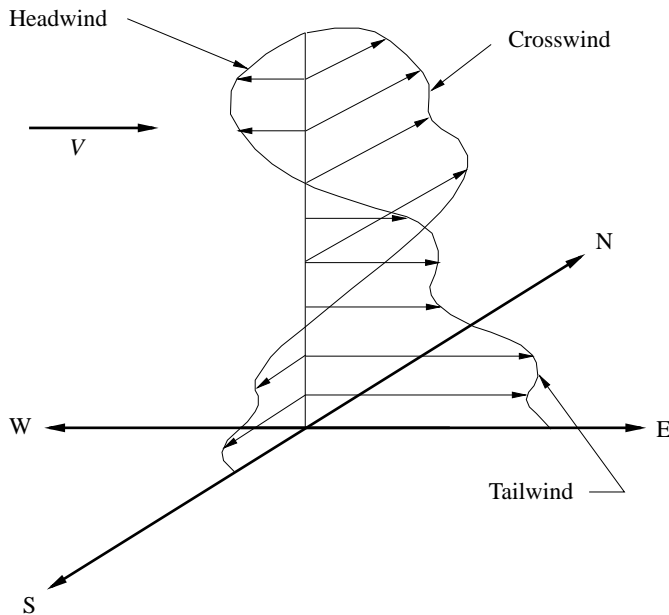


Figure 10: Typical horizontal wind profiles at various altitudes above ground near a thunderstorm

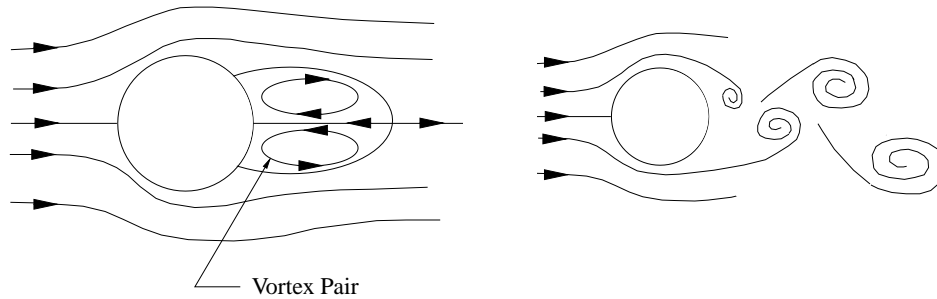
drafts, for aircraft flying at low levels the consequences of the wind fields generated by thunderstorms can be significant.

The large horizontal wind shear associated with these storms can cause a large peak in the aircraft velocity in the direction of flight (see Fig. 10), where the characteristic windspeed wavelength is near the aircraft Phugoid frequency. Since the Phugoid involves an exchange of velocity and altitude, excitation of this mode can cause significant variations in height which must be carefully controlled for both low flying aircraft and aircraft in general when landing. In addition, the effect of a horizontal wind shear in isolation compared to that in conjunction with a downburst can be significantly different, despite the fact that vertical gusts on their own have a much less pronounced effect on aircraft dynamic motion when compared to horizontal gusts.

3.3 Flow past buildings

The study of wind flows past buildings is a subset of the study of incompressible flows about bluff bodies. As such, the various flow regimes likely to be encountered under any given set of atmospheric conditions can be related to the Reynolds number ($Re = (\rho V l) / \mu$). Of particular interest are the low speed, low Reynolds number flow regimes typical of wind speeds past structures on the Earth's surface. In these cases it is the viscosity within the flow which plays a dominant role in determining the size, shape, and properties within the wake behind any submersed body.

At values of $Re \approx 10 - 20$ a pair of stable, symmetric vortices can form behind a body creating a symmetrical flowfield, as illustrated in Fig. 11(a).



(a) Symmetrical vortex pair for $10 \leq Re \leq 20$ (b) von Kármán vortex street $30 \leq Re \leq 5 \times 10^3$

Figure 11: Flows with viscous effects dominant

As the Reynolds number increases to values between 30 and 5×10^3 (depending on the shape of the object, i.e., flat plate, cylinder, etc.) the vortices formed behind the object are shed from the downstream facing surface in an alternating pattern creating what is known as a “von Kármán vortex street” as in Fig. 11(b). It is interesting to note that this structure can also be observed on a very large scale from satellite images of cloud patterns trailing high, isolated mountains (such as those found on islands). In these cases, since both the upper level winds (recall the geostrophic wind) and the size of the length dimension of the island are very large in comparison to the average air viscosity, the apparent Reynolds number would seem to be in excess of the upper limit of approximately 5,000. However, if one substitutes the turbulent eddy viscosity in place of the laminar value to reflect the fact that the mixing on this scale is more dependent on the large scale mechanical motion of the air as opposed to the laminar shear between air molecules, then indeed Re falls within the expected range for exhibiting this type of wake structure.

At even higher Reynolds numbers the inertial factors begin to dominate the flow and the distinct shed vortices can no longer be observed, replaced instead by a turbulent wake (Fig. 12(a)). Between this wake and the smooth flow outside of this region there exists a shear layer of much smaller vortices (Fig. 12(b)). As the Reynolds number is increased even further, or the building length is increased, it is possible to have the wake re-attach to the surface of a building thereby creating a small re-circulation zone immediately downstream of the leading edge in addition to a turbulent wake trailing the structure (Fig. 12(b)).

3.4 Control Algorithms

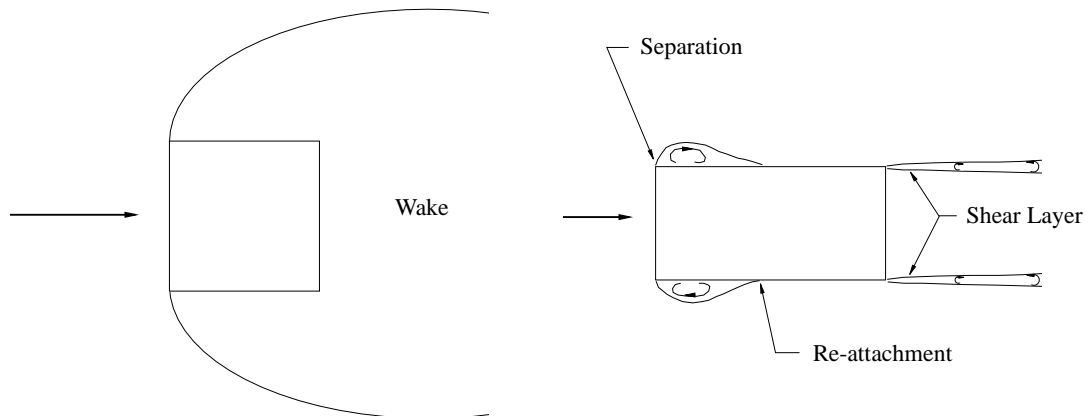
The complete motion of an aircraft is described by a set of twelve, non-linear, ordinary, differential equations: six “dynamic” equations resulting from the application of Newton’s second law in each of the three linear and angular degrees of freedom and six “kinematic” equations resulting from a transformation of reference frames from a body fixed to an Earth fixed, or inertial, reference frame. It is common to simplify these by rephrasing them to reflect small disturbances about a reference condition. This yields the significant result that the equations can be written as two distinct sets of four differential equations, where each set contains only longitudinal or lateral variables thereby decoupling these aircraft modes.

In addition to assuming small disturbances about a reference condition (whose characteristics are specified), it is also common to assume that the aerodynamic forces and moments are linear functions of the derivatives at some initial time t_0 thereby neglecting any unsteady effects (which was the case when considering a linearly varying gust). With these approximations one can write the equations of motion as,

$$\dot{x} = Ax + Bc \tag{44}$$

where x represents a vector of either longitudinal or lateral state variables,

$$x = [\Delta u \ \Delta w \ \Delta q \ \Delta \theta]^T \tag{45}$$



(a) Wake behind a building ($Re \geq 5 \times 10^3$)

(b) Separation/Re-attachment ($Re \gg 5 \times 10^3$)

Figure 12: Flows with inertial effects dominant

$$x = [\Delta v \ \Delta p \ \Delta r \ \Delta \phi]^T \quad (46)$$

In the case of the longitudinal motions the control state vector, c , contains inputs capable of altering any of the variables contained in Eq. 45 (which are generally an elevator deflection (δ_e) or a change in thrust settings (δ_t)). The main control inputs for affecting lateral motion are a change in aileron angle (δ_a) or rudder angle (δ_r), where it should be kept in mind that these are changes in these settings from the values required to maintain the aircraft in the reference condition. In both modes, the matrix A contains the various stability derivatives which are used to linearize the aerodynamic forces and moments, where if all the derivatives with respect to a time rate of change are neglected (i.e. $(\partial M)/(\partial \dot{w}) = M_{\dot{w}} = 0$) one can write,

$$A = \underbrace{\begin{bmatrix} X_u & X_w & 0 & -g \\ Z_u & Z_w & u_o & 0 \\ M_u & M_w & M_q & 0 \\ 0 & 0 & 1 & 0 \end{bmatrix}}_{\text{Longitudinal}} \quad \text{OR} \quad \underbrace{\begin{bmatrix} Y_v & Y_p & (Y_r - u_o) & g \\ L_v & L_p & L_r & 0 \\ N_v & N_p & N_r & 0 \\ 0 & 1 & 0 & 0 \end{bmatrix}}_{\text{Lateral}} \quad (47)$$

while the effect of the controls can be modelled using

$$B = \begin{bmatrix} X_{\delta_e} & X_{\delta_t} \\ Z_{\delta_e} & Z_{\delta_t} \\ M_{\delta_e} & M_{\delta_t} \\ 0 & 0 \end{bmatrix} \begin{bmatrix} \delta_e \\ \delta_t \end{bmatrix} \quad \text{OR} \quad \begin{bmatrix} 0 & Y_{\delta_r} \\ L_{\delta_a} & L_{\delta_r} \\ N_{\delta_a} & N_{\delta_r} \\ 0 & 0 \end{bmatrix} \begin{bmatrix} \delta_a \\ \delta_r \end{bmatrix} \quad (48)$$

In order to incorporate the effects of a gust, it is possible to make use of the gust angular velocity obtained by assuming a linearly varying gust as represented by Eq. 26. In the presence of a gust, the governing equations as represented in Eq. 44 have to be modified slightly,

$$\dot{x} = Ax + Bc + Tg \quad (49)$$

where g now contains the components of the gust vector (Eq. 26) appropriate to the direction of motion under consideration. Therefore, for the longitudinal modes the gust components of interest are u_g , w_g , and q_g while for the lateral modes one must consider v_g , p_g , and both r_{g1} and r_{g2} . The linearization of the aerodynamic forces and moments resulted in expressions for the various quantities of the form (using the change in the pitching moment as an example),

$$\Delta M = M_u \Delta u + M_w \Delta w + M_q \Delta q \quad (50)$$

where in the presence of a gust the relations become,

$$\Delta M = M_u(\Delta u - u_g) + M_w(\Delta w - w_g) + M_q(\Delta q - q_g) \quad (51)$$

This allows the longitudinal and lateral gust matrices multiplying the various components of the vector g to be expressed as,

$$Tg = \begin{bmatrix} -X_u & -X_w & 0 \\ -Z_u & -Z_w & 0 \\ -M_u & -M_w & -M_q \\ 0 & 0 & 0 \end{bmatrix} \begin{bmatrix} u_g \\ w_g \\ q_g \end{bmatrix} \quad (52)$$

or in the lateral direction since there are two distinct gust yaw rates one can write,

$$Tg = \begin{bmatrix} -Y_v & -Y_p & -Y_r \\ -L_v & -L_p & -L_r \\ -N_v & -N_p & -N_r \\ 0 & 0 & 0 \end{bmatrix} \begin{bmatrix} v_g \\ p_g \\ (r_{g1} + r_{g2}) \end{bmatrix} \quad (53)$$

the difference between the two yaw rates stemming from how they are calculated (Eq. 42).

A closer examination of Eq. 49 reveals that if $Bc = -Tg$ then one would completely eliminate the effect of the gust and thus the aircraft would behave as if flying through still air. Such a control input would take the form,

$$c = -B^{-1}Tg \quad (54)$$

where the problem then becomes one of finding the inverse of B . However, from Eq. 48 one can note that this matrix is not square since there are not as many control inputs as there are state variables in either of the two modes of motion. Therefore, even if one were able to measure the gust vector g for use in Eq. 54, it would be impossible to calculate the required inverse without increasing the number of control inputs available.

In practice, gust alleviation is accomplished by choosing one or more variables to be controlled in some manner (held constant, eliminated, minimized, etc.) and designing an algorithm around this goal. For example, with regards to flight through a thunderstorm, it is possible to use tabulated data pertaining to the wind conditions measured during actual storms (similar to the profiles shown in Fig. 10) as gust inputs and calculate elevator and thrust control inputs that would minimize an aircrafts deviation from a given flight path (i.e., a draped surface for low level flying or a glideslope on a landing approach). The accuracy of such methods depends to a large extent on the information assumed available when

developing the control algorithm, where results are likely to be better as more feedback is designed into the system.

Although a complete analysis of the methods available for control system design is beyond the scope of this report, there are numerous references available on the subject (Etkin [4], Nelson [5], or Stevens and Lewis [6]).

References

- [1] Simiu, Emil and Scanlan, Robert H. (1996), *Wind Effects on Structures*, 3 ed, John Wiley and Sons, Inc.
- [2] Amorocho, J. and deVries, J. J. (1980), A New Evaluation of the Wind Stress Coefficient over Water Surfaces, *Journal of Geophysical Res.*, 85, 433–442.
- [3] Holley, W.E. and Jr., A.E. Bryson (1977), Wind Modeling and Lateral Control for Automatic Landing, *Journal of Spacecraft*, 14(2), 65–72.
- [4] Etkin, Bernard and Reid, Lloyd Duff (1996), *Dynamics of Flight*, 3 ed, John Wiley and Sons.
- [5] Nelson, Robert C. (1998), *Flight Stability and Control*, 2 ed, McGraw Hill.
- [6] Stevens, Brian L. and Lewis, Frank L. (2003), *Aircraft Control and Simulation*, 2 ed, John Wiley and Sons, Inc.

List of Acronyms and Symbols

Greek Symbols

α	angle between wind vector and isobars [degrees]
γ	ratio of specific heats
δ	boundary layer height [m], change in control input
θ	Euler angle [degrees]
κ	surface drag co-efficient
λ	gust wavelength [m]
μ	viscosity co-efficient [kg/(m s)], mass ratio
ρ	density [kg/m ³]
σ	root mean square
τ	time [s], shear stress [N/m ²]
ϕ	latitude [degrees], Euler angle [degrees]
ω	angular velocity [rad/s], circular gust frequency [rad/s]
Φ	Power-Spectral Density (psd)
Ω	reduced frequency [rad/m]

Roman Symbols

c	wing chord [m]
$c_{L\alpha}$	lift curve slope of aircraft [/rad]
g	gust velocity vector [m/s], gravitational acceleration [m/s ²]
h	distance perpendicular to the Earth's surface [m]
k	von Kármán constant (≈ 0.4), reduced frequency
l_t	distance from aircraft centre of mass to aerodynamic centre of vertical stabilizer [m]

m	mass [kg]
n	distance parallel to the Earth's surface [m], load factor (L/W)
p	component of angular velocity about the x axis (roll rate) [rad/s], probability
q	component of angular velocity about the y axis (pitch rate) [rad/s]
r	component of angular velocity about the z axis (yaw rate) [rad/s], radius of curvature [m]
s	distance of penetration into a gust [ft]
t	time [s]
u	component of velocity in the x direction [m/s]
u_o	reference condition airspeed [m/s]
v	component of velocity in the y direction [m/s]
w	component of velocity in the z direction [m/s]
z	effective height above ground [m]
z_d	zero plane displacement [m]
z_g	height above ground [m]
z_o	roughness length [m]
F	force [N]
F_g	flight profile alleviation factor
H	distance to maximum magnitude of a discrete gust [ft]
L	component of moment acting in about the x axis [N m], turbulence length scale [ft]
M	component of moment acting in about the y axis [N m]
N	component of moment acting in about the z axis [N m]
Re	Reynolds number
T	time [s], period [s]
U	total gust velocity [ft/s, m/s]

V	velocity [m/s]
V_{gr}	gradient wind velocity [m/s]
V^*	friction velocity [m/s]
W/S	wing loading [kg/m ²]
X	component of force acting in the x direction [N]
Y	component of force acting in the y direction [N]
Z	component of force acting in the z direction [N]

Subscripts

a	aileron
c	coriolis
ds	design gust velocity [ft/s]
e	elevator
fr	friction
g	gust
p	pressure
r	centrifugal, rudder
ref	reference gust velocity [ft/s]
t	thrust

Superscripts

E	with respect to an Earth fixed reference frame
\rightarrow	vector quantity

This page intentionally left blank.

Distribution list

DRDC Ottawa CR 2006-221

Internal distribution

- 1 Giovanni Fusina, DRDC Ottawa
- 1 Paul Hubbard, DRDC Ottawa
- 1 Bumsoo Kim, DRDC Ottawa
- 1 Paul Pace, DRDC Ottawa
- 2 Library

Total internal copies: 6

External distribution

Department of National Defence

- 1 DRDKIM

International recipients

Total external copies: 1

Total copies: 7

This page intentionally left blank.

DOCUMENT CONTROL DATA

(Security classification of title, body of abstract and indexing annotation must be entered when document is classified)

1. ORIGINATOR (the name and address of the organization preparing the document. Organizations for whom the document was prepared, e.g. Centre sponsoring a contractor's report, or tasking agency, are entered in section 8.) J. Etele, Mechanical and Aerospace Engineering Department, Carleton University 1125 Colonel By Drive, Ottawa, Ontario, Canada, K1S-5B6		2. SECURITY CLASSIFICATION (overall security classification of the document including special warning terms if applicable). UNCLASSIFIED	
3. TITLE (the complete document title as indicated on the title page. Its classification should be indicated by the appropriate abbreviation (S,C,R or U) in parentheses after the title). Overview of Wind Gust Modelling with Application to Autonomous Low-Level UAV Control			
4. AUTHORS (last name, first name, middle initial) Etele, J.			
5. DATE OF PUBLICATION (month and year of publication of document) November 2006		6a. NO. OF PAGES (total containing information. Include Annexes, Appendices, etc). 42	6b. NO. OF REFS (total cited in document) 6
7. DESCRIPTIVE NOTES (the category of the document, e.g. technical report, technical note or memorandum. If appropriate, enter the type of report, e.g. interim, progress, summary, annual or final. Give the inclusive dates when a specific reporting period is covered). Contract Report			
8. SPONSORING ACTIVITY (the name of the department project office or laboratory sponsoring the research and development. Include address). Defence R&D Canada – Ottawa 3701 Carling Avenue, Ottawa, Ontario, Canada K1A 0Z4			
9a. PROJECT NO. (the applicable research and development project number under which the document was written. Specify whether project). ARP 13jc		9b. GRANT OR CONTRACT NO. (if appropriate, the applicable number under which the document was written). L5-41768	
10a. ORIGINATOR'S DOCUMENT NUMBER (the official document number by which the document is identified by the originating activity. This number must be unique.) DRDC Ottawa CR 2006-221		10b. OTHER DOCUMENT NOS. (Any other numbers which may be assigned this document either by the originator or by the sponsor.)	
11. DOCUMENT AVAILABILITY (any limitations on further dissemination of the document, other than those imposed by security classification) (X) Unlimited distribution () Defence departments and defence contractors; further distribution only as approved () Defence departments and Canadian defence contractors; further distribution only as approved () Government departments and agencies; further distribution only as approved () Defence departments; further distribution only as approved () Other (please specify):			
12. DOCUMENT ANNOUNCEMENT (any limitation to the bibliographic announcement of this document. This will normally correspond to the Document Availability (11). However, where further distribution beyond the audience specified in (11) is possible, a wider announcement audience may be selected).			

13. ABSTRACT (a brief and factual summary of the document. It may also appear elsewhere in the body of the document itself. It is highly desirable that the abstract of classified documents be unclassified. Each paragraph of the abstract shall begin with an indication of the security classification of the information in the paragraph (unless the document itself is unclassified) represented as (S), (C), (R), or (U). It is not necessary to include here abstracts in both official languages unless the text is bilingual).

The Future Forces Synthetic Environmentn (FFSE) Section at Defence R&D Canada - Ottawa is currently embarked on an Advanced Research Program entitled "Synthetic Environment Support to Uninhabited Aerial Vehicles (UAVs)". As part of this project, FFSE has already developed an agile, versatile synthetic environment (SE) tailored toward UAV operations. An enhancement to this SE is being investigated, whereby wind gusts in urban and mountainous environments and their resulting effect on the UAV flight path will be integrated in the FFSE UAV SE. This will give FFSE's Clients a realistic understanding of the environmental issues associated with UAV operations in urban and mountainous environments and aid in concept of operations development. It will also form the basis of designing control algorithms to alleviate the UAV's susceptibility to wind gusts. This present study reviews methods available to both quantify a wind gust and use this quantification in the prediction of its effect on UAV stability.

14. KEYWORDS, DESCRIPTORS or IDENTIFIERS (technically meaningful terms or short phrases that characterize a document and could be helpful in cataloguing the document. They should be selected so that no security classification is required. Identifiers, such as equipment model designation, trade name, military project code name, geographic location may also be included. If possible keywords should be selected from a published thesaurus. e.g. Thesaurus of Engineering and Scientific Terms (TEST) and that thesaurus-identified. If it not possible to select indexing terms which are Unclassified, the classification of each should be indicated as with the title).

wind gust modelling
UAV stability and control

Defence R&D Canada

Canada's leader in Defence
and National Security
Science and Technology

R & D pour la défense Canada

Chef de file au Canada en matière
de science et de technologie pour
la défense et la sécurité nationale



www.drdc-rddc.gc.ca